



Infinite Boundary Element Formulation for the Analysis of Half-space Problems

H. Ashrafi¹, M. R. Hematyan², M. Kasraei³

1,3- Department of Mechanical Engineering of Agricultural Machines, Shiraz University, Shiraz, Iran

2- Department of Mechanical Engineering, Shiraz University, Shiraz, Iran

hosseynashrafi@gmail.com

Abstract

Special type of boundary elements are discussed which can be used for the modeling of surfaces where extended to infinity (half-space). The theoretical background and details of implementation are discussed. The decay function for stress analysis is then developed based on the theoretical displacement reduction away from the source of loading. Effective order-adaptive criteria are used for numerical integration of the integrals over the infinite boundary elements. On numerical example, a practical application for the use of these elements to modeling of rectangular foundation is provided.

Keywords: Infinite boundary elements, Half-space problems, Numerical integration.

Introduction

During recent years, the boundary element method has found considerable applications in the solution of engineering problems, such as contact mechanics, elastoplasticity, elastodynamics, fracture mechanics and geomechanics. More importantly, the problems that once seemed completely inflexible for an analytic study can now be analyzed by this technique rather easily. The boundary element method is ideally suited for the analysis of problems involving an infinite domain because only the problem surface has to be discretized and the conditions at infinity are automatically satisfied by the fundamental solution. However, the region of interest of many engineering problems extends to infinity. In some cases, we encounter problems in which the surface to be discretized also extends to infinity. This creates difficulties for numerical methods, such as the finite element method, which are based on finite domain discretization, however the advent of 'infinite element' methodologies [1]. In the same way as in the finite element method these problems can be solved by truncating the boundary element mesh at a large distance away from the zone of interest. The disadvantage of such approach is that a large number of boundary elements may be used for modeling the remote surface and that an unknown error may be introduced if the truncation occurs too near to the zone of interest. So, boundary element method also shows parallel deficiencies if the basic Kelvin fundamental solution satisfies far-field boundary conditions different from those of the boundary value problem. Clearly, analysis of half-space problems by the BEM, using the full-space Kelvin's functions, requires discretization of the free-surface of the problem domain. The semi-infinite surface is normally truncated to a bounded region of manageable size, but to obtain acceptable results convergence studies are necessary and these are unavoidably inefficient in terms of resources. A much more effective method is to incorporate infinite elements into the boundary element analysis.

Infinite elements have been used for the modeling of infinite surfaces in boundary element discretizations since 1979s. The principal idea to deal with these problems for the using of infinite boundary elements was first suggested by Watson [2]. Afterwards was employed by Beer et al. [3] to model a small region of a very long tunnel which was assumed to extend to infinity. Beer and Watson [4] discussed the application of special types of boundary elements for the modeling of surfaces which extend to infinity. They excellently discussed about the approach of mapping infinite surfaces to a unit square and also shown suitable functions for describing the decay of displacements and tractions in the infinite direction depending on the type of problem to be analyzed. Zhang et al. [5] developed shape functions for describing far-field multiple wave propagation. Kaljevic et al. [6] presented an infinite boundary element for the analysis of three-dimensional potential problems in an unbounded medium. They did infinite boundary element formulations to allow their coupling with the finite element matrices for

1- M.Sc. Student of Shiraz University.

2- Assistant Professor of Shiraz University.

3- Assistant Professor of Shiraz University.



finite domains and to obtain the overall matrices without destroying the banded structure of the FE matrices. They divided infinite body into a number of zones whose contributions expressed in terms of the nodal quantities at FE nodes by employing suitable decay functions and performing mainly analytical integrations of the boundary element kernels. Parreira and Pereira Almeida [7] discussed the application of the recently developed algorithms for the direct numerical evaluation of the strongly singular integrals to semi-infinite special fundamental solutions and to infinite boundary elements. Liu and Farris [8] presented a three-dimensional infinite boundary element method for the modeling of half-space contact problems. They discretized infinite surface of the half-space into a finite number of elements with the elements extending to infinity mapped onto finite elements and then special mapping scheme that handles the singular integrals over those infinite boundary elements introduced. This infinite boundary element scheme treated the effect of infinity correctly, leading to excellent accuracy which was verified for a half-space subjected to uniform pressure in a circular region and a square region on the surface. Davies and Bu [9] presented details of a novel infinite boundary element approach for the half-space problems, which is applicable to, in principle, any function which decays in the far-field. They derived an efficient approach for numerical integration to infinite boundary elements. Bu [10] also analyzed axisymmetric half-space problems by extending previous work on infinite boundary elements. He then developed a condensation process which could considerably reduce the dimensions of system matrices and computational time. Liang and Liew [11] proposed an effective solution technique which used alternative fundamental solutions of the half-space (Mindlin's solution) and full space (Kelvin's solution) problems. They avoided from the singular line integrals in the proposed solution technique, while the discretization of infinite elements is independent of the finite boundary elements. Xiao and Wang [12] presented the infinite element method for 3-D boundary element analysis of half-space problems. They used displacement decay function to represent far-field displacement and also derived the efficient adaptive integration for numerical integration.

The scope of this paper is to discuss the theoretical background and implementation of the effective infinite boundary elements in much more details. In particular, a semi-analytical approach based on a circular region of exclusion is developed in order to circumvent difficulties in numerical integrations in the far-field. The mapping techniques and the order-adaptive criteria discussed for the numerical integrations. The example is shown which demonstrate that the elements perform very effective.

Numerical Discretization and Mapping

The Boundary Element Method is the numerical method of solution for boundary integral equations based on a discretization procedure. The first step in the discretization is to divide the boundary S into many elements. The discretization of the unbounded domain and mapping of the infinite elements into Gaussian integration space are very considerable. Many difficulties can appear in the geometrical representation of the infinite elements, especially if the infinite elements are not bounded by rays from a source point since this can lead to non-unique mapping and other problems [1]. The boundary of the half-space model is divided into a core region S_F , the far-field S_I , and the hemispherical surface S_H (with radius extending to infinity for modeling half-space), as shown in Figure 1. The core region is discretized with K quadrilateral boundary elements of quadratic serendipity family, in which the geometry and field quantities are described by quadratic shape functions N_a . The far field is modeled by means of infinite boundary elements whose edges, in the radial direction, are defined by straight lines radiating from the centre of the source region, shown schematically in Figure 2. Over each infinite element, the shape function in the radial direction is described by the decay function D which is introduced later. The hemispherical surface need not be discretized since the displacements and tractions are zero (regularity conditions [13]).

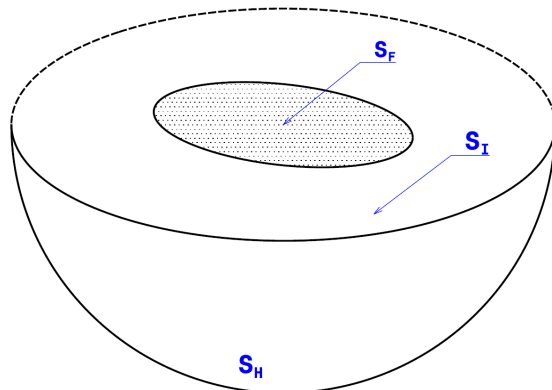


Figure 1: The half-space model.

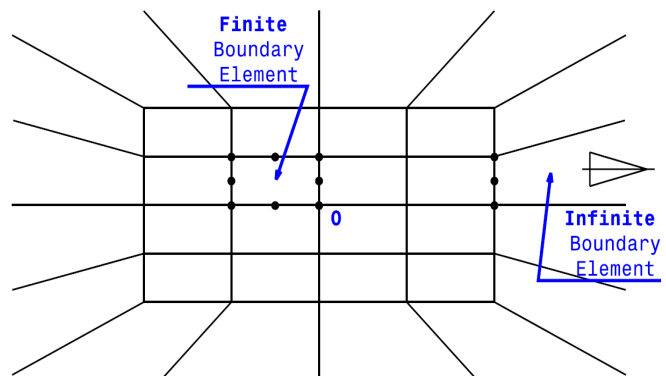


Figure 2: Discretization of the model into finite and infinite boundary elements.

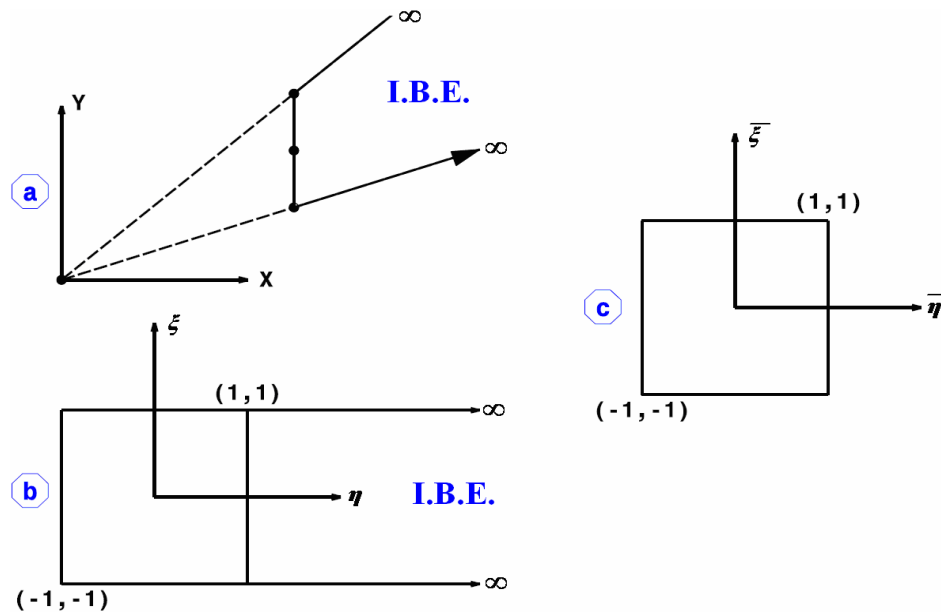


Figure 3: Mapping of an infinite boundary element. (a) Infinite element in X-Y space, (b) Infinite element in $\eta - \xi$ space, (c) infinite element in $\bar{\eta} - \bar{\xi}$ space.

As shown in Figure 3a, an infinite region is defined by the rays originating from the source region and extending to infinity. The infinite region is then mapped to a square with the η -direction extending to infinity (Figure 3b). The geometry parameters are then approximated using the shape functions M_α , which is:

$$\begin{aligned} x &= \frac{1+\eta}{2} \sum_{\alpha=1}^3 M_\alpha(\xi) x_\alpha \\ y &= \frac{1+\eta}{2} \sum_{\alpha=1}^3 M_\alpha(\xi) y_\alpha \end{aligned} \quad (1)$$

where x_α and y_α are the coordinates of nodal points, and M_α are the quadratic shape functions, where defined as:

$$M_1 = \frac{\xi(\xi-1)}{2}, \quad M_2 = 1 - \xi^2, \quad M_3 = \frac{\xi(\xi+1)}{2} \quad (2)$$

To facilitate numerical integration, infinite elements are mapped into a finite region of intrinsic coordinate space. Here, nodes are placed at $\eta = -1, 0$ and 1 , but η varies from -1 to infinity. A further mapping of the infinite element ($\eta \geq 1$) is then transformed from the local coordinate (η, ξ) to the coordinate $(\bar{\eta}, \bar{\xi})$ with range $(-1, 1)$, as shown in Figure 3c. The corresponding transformation after some operations can be written as [2, 4]:

$$\eta = \frac{3\bar{\eta} + 5}{1 - \bar{\eta}}, \quad \xi = \bar{\xi} \quad (3)$$

By substituting equation (3) into equation (1), the suitable coordinate transformation for the infinite boundary element is given by:

$$\begin{aligned} x &= \left(\frac{3 + \bar{\eta}}{1 - \bar{\eta}} \right) \sum_{\alpha=1}^3 M_\alpha x_\alpha \\ y &= \left(\frac{3 + \bar{\eta}}{1 - \bar{\eta}} \right) \sum_{\alpha=1}^3 M_\alpha y_\alpha \end{aligned} \quad (4)$$

For these infinite elements, the transformation from the global Cartesian system (x, y) to a system $(\bar{\eta}, \bar{\xi})$ defined over the surface of the problem is given by a Jacobian matrix (J) that can be computed without special difficulty. It should be mentioned that $(1 - \bar{\eta})$ is of order $O(r^{-1})$ and consequently, J is of order $O(r^3)$.

It should be also mentioned that this mapping method puts the integration points on lines radiating from the origin and concentrated near to the source region owing to improves the accuracy of numerical integration.



Decay Functions to Modeling the Far-field Behavior

For the isoparametric boundary elements, the variation of the displacement \mathbf{u} and tractions \mathbf{t} is determined from the values at the nodes \mathbf{u}_α and \mathbf{t}_α using interpolation functions which are the same as the shape functions used to describe the element geometry. However, for the 3-D infinite boundary elements, this variation is approximated by means of isoparametric interpolation in the finite direction ξ and decay functions D_u and D_t in the infinite direction:

$$\begin{aligned} \mathbf{u} &= \frac{1+\eta}{2} \sum_{\alpha=1}^3 M_\alpha(\xi) D_u(\eta) \mathbf{u}_\alpha \\ \mathbf{t} &= \frac{1+\eta}{2} \sum_{\alpha=1}^3 M_\alpha(\xi) D_u(\eta) \mathbf{t}_\alpha \end{aligned} \quad (5)$$

Displacements and tractions decay along the infinite direction of a half-space. In the analysis of half-space problems, boundary elements need only be specified on the surface of the semi-infinite domain. In the other hand, this unbounded surface in the far-field satisfies regularity conditions, which makes it possible to simplify the boundary integral equations. Thus, in stress analysis, it only becomes necessary to develop representations of the displacements into the far-field. Various approaches are possible to describe the decay of far-field quantities. Here, the Boussinesq solution indicates that the decay of the displacement should be of order $O(r^{-1})$ and that of the tractions of order $O(r^{-2})$, where r is the radial distance from the decay origin to any arbitrary point [4].

For 3-D static stress analysis, the decay function only for displacements takes the simple form [9-12]:

$$D_u = \frac{r_0}{r} \quad (6)$$

which is unity at some arbitrary reference point r_0 where it is the radial distance along the free surface from the source of disturbance to the reference point and r is the radial distance to any arbitrary collinear point in the far-field, with the condition that ($r \geq r_0$). The decay function takes the same role of a shape function in the radial direction, interpolating between the value of the field quantity at an appropriate reference point in the near-field, at ($r = r_0$), and the value of zero in infinity, at ($r = \infty$). After some manipulations, it can be shown that the decay function can be introduced in the coordinate system $(\bar{\eta}, \bar{\xi})$ as follows:

$$D_u = \frac{r_0}{r} = \frac{1-\bar{\eta}}{3+\bar{\eta}} \quad (7)$$

Implementation of Direct Boundary Integral Equations

The boundary integral equation for linear elastostatic problems can be derived based on Betti's reciprocal work theorem [13, 14]. For implementation of the 3-D stress analysis, the displacement boundary integral equations in the absences of body forces, can be written as:

$$C_{ij}(x') u_j(x') + \int_S T_{ij}(x', x) u_j(x) dS = \int_S U_{ij}(x', x) t_j(x) dS \quad (8)$$

where S is the boundary of the problem domain; $x, x' \in S$ are the field and source points; T_{ij} and U_{ij} are the traction and displacement fundamental solutions; the free term C_{ij} is a (3×3) matrix that is a function of the boundary geometry near of x' and the Poisson's ratio which obtaining from the treatment of the improper surface integral involving T_{ij} [13]; u_j and t_j are the actual displacements and tractions. The analytical solution of the boundary integral equations is only possible for relatively simple problems and so, it is necessary to implement these equations using a numerical method.

Using the discretization scheme described above, the discretized boundary element formulation involving infinite boundary elements can be expressed in the following form:

$$\begin{aligned} C_{ij} u_j + \sum_{\alpha=1}^8 \sum_K u_{j\alpha} \int_{S_F} T_{ij} N_\alpha dS + \sum_{\alpha} \sum_{K^*} u_{j\alpha} \int_{S_F} T_{ij} N_\alpha dS + \sum_{K^*} u_{j\alpha^*} \int_{S_F} T_{ij} N_{\alpha^*} dS \\ + \sum_{\alpha=1}^3 \sum_K u_{j\alpha} \int_{S_I} T_{ij} M_\alpha D_u dS + \sum_{\alpha} \sum_{K^*} u_{j\alpha} \int_{S_I} T_{ij} M_\alpha D_u dS + \sum_{K^*} u_{j\alpha^*} \int_{S_I} T_{ij} M_{\alpha^*} D_u dS \\ = \sum_{\alpha=1}^8 \sum_K t_{j\alpha} \int_{S_F} U_{ij} N_\alpha dS + \sum_{\alpha=1}^8 \sum_{K^*} t_{j\alpha} \int_{S_F} U_{ij} N_\alpha dS \end{aligned} \quad (9)$$

in which the superscripts of \wedge and $*$ refer to nonsingular and singular quantities, respectively; F and I refer to finite and infinite regions; K and α also refer to elements and nodes. It should be noted that only the infinite region integrals over the free surface which involve the traction kernel need to be included in equation (9).



At this part, at first, we consider the five finite region integrals. The first three terms at the left side refer to the strongly singular traction fundamental solution while the two terms of the right side refer to the weakly singular displacement fundamental solution. The weakly singular fundamental solution is concerned in two terms; the first of them refers to nonsingular integrals while the second term refers to the singular integrals. The strongly singular fundamental solution is included the singular integrations into two parts: the first part involves singular integrations in which the source point is not coincident with the current node of the field element and the second part is not integrable by normal means. Only the infinite region integrals over the free surface which involve the strongly singular integrals require to be included in equation (9). Therefore, the corresponding infinite region integrals involving the weakly singular fundamental solution are zero owing to regularity conditions, and all other integrals over the hemispherical boundary (S_H) tend to zero in the limit [13]. The integrals in equation (9) can be computed using Gaussian quadrature technique except for the two following strongly singular integrals (that mentioned before):

$$\sum_{K^*} u_{j\alpha^*} \int_{S_F} T_{ij} N_{\alpha^*} dS, \quad \sum_{K^*} u_{j\alpha^*} \int_{S_1} T_{ij} M_{\alpha^*} D_u dS \quad (10)$$

These strongly singular integrals and the free term C_{ij} can be determined by indirect method by noting that, for a body undergoing rigid body motion, all of the boundary tractions are zero [2-4, 14]. At this paper, this approach is extended to unbounded domains by analytical evaluating the integrals over the infinite boundary of the half-space except for the free surface. However, for evaluating the strongly singular integral over S_1 , it is necessary to partition it into two parts since it is incompatible with the rigid body motion condition owing to containing the decay function, so:

$$\int_{S_1} T_{ij} M_{\alpha^*} D_u dS = \int_{S_1} T_{ij} M_{\alpha^*} dS + \int_{S_1} T_{ij} M_{\alpha^*} (D_u - 1) dS \quad (11)$$

in which the first integral on the right side can be dealt with using the rigid body motion method while the second is now only weakly singular and can be evaluated by normal means.

According to mentioned method, for unit translation, equation (8) changes to [13, 14]:

$$C_{ij} = - \int_S T_{ij} dS = - \int_{S_F} T_{ij} dS - \int_{S_1} T_{ij} dS - \int_{S_H} T_{ij} dS \quad (12)$$

The discretized form of above equation can be written as:

$$C_{ij} + \sum_{K^*} \int_{S_F} T_{ij} N_{\alpha^*} dS + \sum_{K^*} \int_{S_1} T_{ij} M_{\alpha^*} dS = - \sum_{\alpha} \sum_{K^*} \int_{S_F} T_{ij} N_{\alpha} dS - \sum_{\alpha} \sum_{K^*} \int_{S_1} T_{ij} M_{\alpha} dS - \sum_{\bar{K}} \int_{S_F} T_{ij} dS - \sum_{\bar{K}} \int_{S_1} T_{ij} dS + \frac{\delta_{ij}}{2} \quad (13)$$

in which the four integral terms on the right side of equation represent the remaining singular integrals for both the finite and infinite regions. The last term is the analytical value of the azimuthal integral over S_H , which is independent of the radius of the hemisphere [10].

Although the integrals over the infinite domain on the right side of equation (13) are integrable, they are unbounded if the integration is carried out element by element, which it makes difficulties.

Numerical Integration

Two types of integrals, singular and nonsingular, are involved in the boundary element analysis, depending on whether the field point places in the element being integrated or not. The nonsingular integrals over finite regions can be evaluated numerically. Since the traction fundamental solution is of order $O(r^{-2})$ and the Jacobian matrix is of order $O(r^3)$ and the displacement decay function is of order $O(r^{-1})$, the nonsingular integrals in equation (13) are bounded as $r \rightarrow \infty$. To develop an order-adaptive scheme for the numerical integration of these nonsingular integrals, a series of numerical tests has been performed by computing the integral $\int (D/r^2) dS$ over an infinite element. For each source point, the integrals were computed using a sequence of Gauss-Legendre formulae up to the eleventh order, and these were then compared with the analytical solutions. Clearly, for a specified precision, the minimum necessary integration order depends on the distance from the source point to the region of integration. These tests suggested that nonsingular integrals over infinite boundary elements can be evaluated accurately using 9×3 integration order in the radial and the circumferential directions, respectively [10]. The integrable singular integrals over quadratic boundary elements are carried out using triangular transformation [15]. Integrable singular integrals over infinite boundary elements can be computed by subdividing the integral domain into a singular finite region and an infinite nonsingular region. Both integrals can be easily carried out using the above mentioned methods.

It should be noted that again, the infinite region integrals in equation (13) cannot be calculated numerically if the integrations are carried out element by element since these subintegrals are unbounded [4, 10]. In principle,



numerical integration over the entire region could be done but this process would be slowly convergent and time consuming. Consequently, this difficulty has been solved analytically by the exploiting the antisymmetry of the traction fundamental solution over the complete semi-infinite surface, rather than considering individual infinite elements. As shown in Figure 4, the far-field is subdivided into two regions, S_1 and S_2 , defined by a circle of radius ρ centered at the current source point. Each infinite boundary element is then divided into a finite subelement (bounded by the circle and S_F) and an infinite region, which the union of all of the latter is S_2 . The finite subelements, which together comprise the region S_1 exterior to S_F are geometrically similar to the finite boundary elements and can be computed without special difficulty using the same methods. The symmetry of S_2 has made it possible to perform the integration over this infinite subregion analytically for polar coordinates. After some operations [10], it is found that only the diagonal block of the integral, matrix P_{ij} , is different from zero. The nonzero elements of this integral are as follows:

$$\begin{aligned}
 P_{11} &= \frac{(4\nu-5)(y_3-x_3)}{8\rho(1-\nu)} \\
 P_{22} &= P_{11} \\
 P_{33} &= \frac{-3\rho^2(1-2\nu)(y_3-x_3)-(y_3-x_3)^3}{12\rho^3(1-\nu)}
 \end{aligned}
 \tag{14}$$

in which x_3 and y_3 are the z -coordinates of the source point and the far-field region, respectively. Clearly these values are bounded and are identically zero for $\rho \rightarrow \infty$. The right side integrals of equation (13) involving the infinite elements can now be written as the sum of the integrals over S_1 and S_2 , as follows:

$$\sum_{\bar{\alpha}} \sum_{K^*} \int_{S_1} T_{ij} M_{\bar{\alpha}} dS + \sum_K \int_{S_1} T_{ij} dS = \sum_{\bar{\alpha}} \sum_{K^*} \int_{S_1} T_{ij} M_{\bar{\alpha}} dS + \sum_K \int_{S_1} T_{ij} dS + P_{ij}
 \tag{15}$$

Clearly, as noted above, these integrals over S_1 can be evaluated without difficulty.

Assembly of System of Equations

By allowing the source point to coincide sequentially with all nodal points on the boundary, the matrix form of the global system of boundary integral equations can be expressed as:

$$\mathbf{H} \mathbf{u} = \mathbf{G} \mathbf{t}
 \tag{16}$$

where \mathbf{u} and \mathbf{t} are the displacement and traction vectors for all the nodes, respectively. The \mathbf{H} and \mathbf{G} are coefficient matrices containing the appropriate contributions of the surface integrals of T_{ij} and U_{ij} .

Substitution of the known boundary conditions yields the remaining unknowns using standard matrix solution procedures. After introducing the prescribed boundary conditions, the final system of equations is obtained by interchanging columns in the matrices \mathbf{H} and \mathbf{G} to gather all unknowns into the vector \mathbf{X} on the left hand side as follows:

$$\mathbf{A} \mathbf{X} = \mathbf{F}
 \tag{17}$$

The above system of equations is fully populated and nonsymmetric which can be solved by computer software.

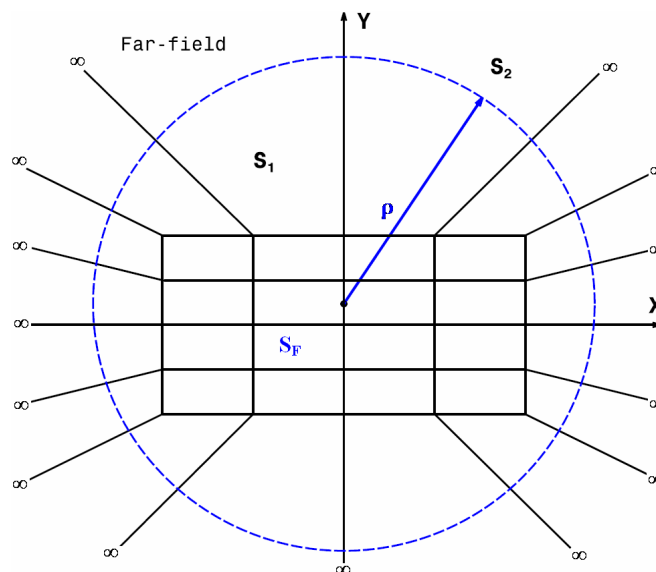


Figure 4: The division of the half-space surface into two regions.



Numerical Model Results

The vertical displacement (u) of a half-space due to a uniformly distributed load of unit intensity (P) acting on an area of square foundation with the surface of side $2a$ is verified. The elastic half-space defined by its shear modulus G and Poisson's ratio ν and also the foundation is assumed to be smooth and negligible flexural rigidity for the purpose of this analysis. Schematic of the model has been presented in Figure 5.

The foundation was discretized using only 2×2 quadratic finite boundary elements. Results of the calculation of vertical dimensionless displacement are presented in Figures 6 and 7 for three different types of meshes. The dimensionless displacement is introduced as uG/Pb owing to better comparison.

1. Finite region type (1) – At this mesh, the foundation is discretized with four elements (63 DOF). This scheme corresponds to the inner four elements shown in Figure 2.
2. Finite region type (2) – At this type, the foundation and a ring of finite-size boundary elements around the foundation are discretized. The truncated mesh has dimensions $2a \times 2a$ i.e. the ring of traction-free elements around the foundation are of dimension $a \times a$. This type has 16 elements with 195 DOF. This scheme corresponds to the inner 16 elements shown in Figure 2.
3. Infinite region – the near-field of the region is discretized as in (2). The far-field is discretized into 16 infinite elements, defined by the rays through the end-nodes of the edges of the elements on the near-field boundary (Fig. 2). Introduction of these elements does not certainly increase the number of degrees of freedom (32 elements, 195 DOF).

These results are compared with the exact analytical solution [16] as shown in Figures 6 and 7.

Conclusion

The theoretical basic and implementation of the effective infinite boundary elements are discussed. It is shown that these elements can be used for modeling surfaces which extend to infinity as encountered in the analysis of half-space problems.

The implementation of the algorithm contains a number of features, including the treatment of the strong singularities for the half-space by an extension of the finite region rigid-body motion approach, the analytical integration of the azimuthal integral over the half-space for embedded sources, and the integration of the unbounded infinite integrals by invoking circular regions of exclusion.

References

1. Bettess, P. (1992) *Infinite Elements*. Penshaw Press, Sunderland, UK.

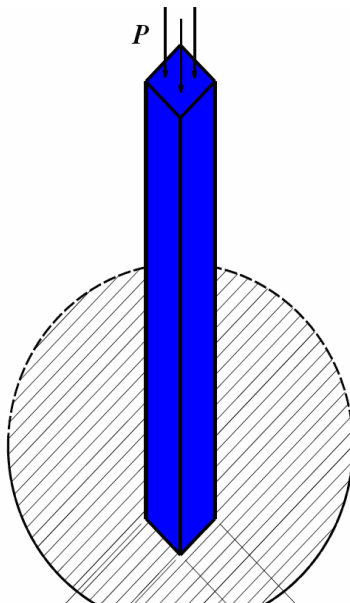


Figure 5: Schematic of the model.

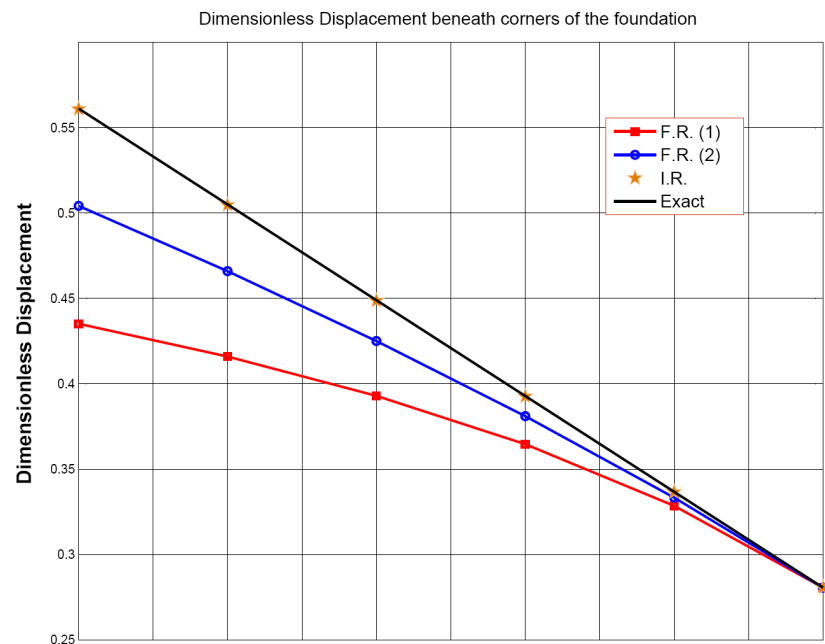


Figure 6: Dimensionless displacement beneath corners of the foundation.

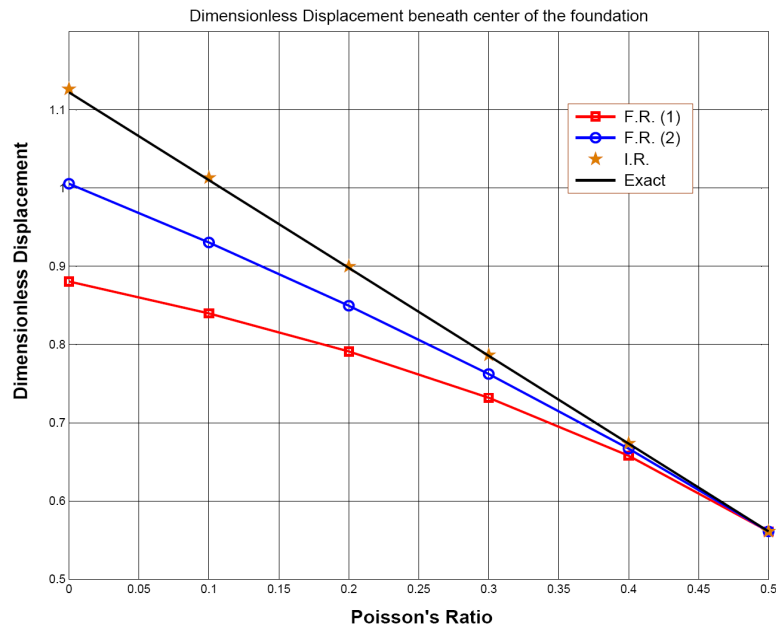


Figure 7: Dimensionless displacement beneath center of the foundation.

2. Watson, J.O. (1979) Advanced implementation of the boundary element method for two- and three-dimensional elastostatics. *Developments in Boundary Element Methods-1*, eds. Banerjee, P.K. and Butterfield, R., Applied Science, London, 31–63.
3. Beer, G. Watson, J.O. and Swoboda, G. (1987) Three-dimensional analysis of tunnels using infinite boundary elements. *Computers and Geotechnics*, **3**, 37–58.
4. Beer, G. and Watson, J.O. (1989) Infinite boundary elements. *International Journal for Numerical Methods in Engineering*, **28**, 1233–1247.
5. Zhang, C. Song, C. and Pekau, O.A. (1991) Infinite boundary elements for dynamic problems of 3-D half space. *International Journal for Numerical Methods in Engineering*, **31**, 447–462.
6. Kaljevic, I. Saigal, S. and Ali, A. (1992) Infinite boundary element formulation for three-dimensional potential problems. *International Journal for Numerical Methods in Engineering*, **35**, 2079–2100.
7. Parreira, P. and Pereira, A.O. (1993) Infinite boundary elements with direct evaluation of Cauchy principal value integrals. *Boundary Elements XV: Fluid Flow and Computational Aspects*, 469–482.
8. Liu, M. and Farris, T.N. (1993) Three-dimensional infinite boundary elements for contact problems. *International Journal for Numerical Methods in Engineering*, **36**, 3381–3398.
9. Davies, T.G. and Bu, S. (1996) Infinite boundary elements for the analysis of halfspace problems. *Computers and Geotechnics*, **19**(2), 137-151.
10. Bu, S. (1996) 3D boundary element analysis of axisymmetric halfspace problems. *Engineering Analysis with Boundary Elements*, **17**, 78–84.
11. Liang, J. and Liew, K.M. (2001) Boundary elements for half-space problems via fundamental solutions: A three-dimensional analysis. *International Journal for Numerical Methods in Engineering*, **52**, 1189–1202.
12. Xiao, H.T. and Wang, X.M. (2004) Infinite boundary elements for analysis of half-space problems. *Rock and Soil Mechanics*, **25**, 91–94.
13. Aliabadi, M.H. (2002) *The Boundary Element Method (Applications in Solids and Structures)*. John Wiley and Sons, Chichester, UK.
14. París, F. and Cañas, J. (1997) *Boundary Element Method (Foundations and Applications)*. Oxford University Press, New York, USA.
15. Aliabadi, M.H. Hall, W.S. and Hibbs, T.T. (1987) Exact singularity canceling for the potential kernel in the boundary element method. *Communications in Appl. Num. Meth.*, **3**, 123–128.
16. Poulos, H.G. and Davis, E.H. (1974) *Elastic Solutions for Soil and Rock Mechanics*. John Wiley and Sons, New York, USA.